Behavioral/Systems/Cognitive

Vocal Premotor Activity in the Superior Colliculus

Shiva R. Sinha[1,3] **and Cynthia F. Moss**[1,2,3]

[1]Neuroscience and Cognitive Science Program, [2]Institute for Systems Research, [3]Department of Psychology, University of Maryland, College Park, Maryland 20742

Chronic neural recordings were taken from the midbrain superior colliculus (SC) of echolocating bats while they were engaged in one of two distinct behavioral tasks: virtual target amplitude discrimination (VTAD) and real oscillating target tracking (ROTT). In the VTAD task, bats used a limited range of sonar call features to discriminate the amplitude category of echoes, whereas in the ROTT task, the bat produced dynamically modulated sonar calls to track a moving target. Newly developed methods for chronic recordings in unrestrained, behaving bats reveal two consistent bouts of SC neural activity preceding the onset of sonar vocalizations in both tasks. A short lead bout occurs tightly coupled to vocal onset (VTAD, −5.1 to −2.2 ms range, −3.6 ± 0.7 ms mean lead time; ROTT, −3.0 to + 0.4 ms range, −1.2 ± 1.3 ms mean lead time), and this activity may play a role in marking the time of each sonar emission. A long lead bout in SC activity occurs earlier and spreads over a longer interval (VTAD, −40.6 to −8.4 ms range, −22.2 ± 3.9 ms mean lead time; ROTT, −29.8 to −7.1 ms range, −17.5 ± 9.1 ms mean lead time) when compared with short lead events. In the goal-directed ROTT task, the timing of long lead event times vary with the bat's sonar call duration. This finding, along with behavioral studies demonstrating that bats adjust sonar call duration as they track targets at changing distance, suggests the bat SC contributes to range-dependent adjustments of sonar call duration.

Key words: **colliculus; premotor; extracellular recording; vocalization; spatial orientation; sensorimotor; neuroethology**

Introduction

Echolocating bats have evolved a biological sonar system that enables them to orient and forage in darkness. Bats emit temporally dynamic sequences of sonar vocalizations and process information carried by returning echoes to determine the position, size, and features of objects (Griffin, 1958; Simmons, 1973; Moss and Schnitzler, 1995). Similar to whisking in rodents or eye movements in primates, echolocation is an adaptive behavior: the echolocating bat rapidly modifies the duration, production rate, and spectrum of its sonar vocalizations in response to changes in target location (Griffin et al., 1960; Surlykke and Moss, 2000; Smotherman et al., 2003) (see Fig. 1*A*).

The midbrain superior colliculus (SC) is implicated in orienting behaviors in a variety of species. Comparative animal studies suggest a role for the SC in shaping saccadic (Robinson, 1972; Sparks, 2002), smooth-pursuit (Krauzlis, 2004), and vergence (Gnadt and Beyer, 1998; Chaturvedi and Van Gisbergen, 1999) eye movements in monkeys, control of the head, eyes, and pinna in cat (Guitton and Munoz, 1991; Stein and Meredith, 1993), and in orienting and evasive behaviors in rat (Dean et al., 1989). Other studies have identified specializations of the optic tectum (the nonmammalian SC homolog) that support head turning in barn owl (du Lac and Knudsen, 1990), snapping, body, and head turning behaviors in frog (Ewert, 1997), head orienting in rattlesnakes (Hartline et al., 1978; Dacey and Ulinski, 1986), and tail, head, and eye movements in goldfish (Herrero et al., 1998). These diverse behaviors are mediated by several pathways from the SC to the brainstem nuclei, which transform SC signals and projects to motor neurons mediating orienting behaviors (Masino and Knudsen, 1990; Moschovakis et al., 1996).

For the echolocating bat, biologically relevant SC specializations have been reported, which are proposed to play a role in three-dimensional (3-D) auditory localization (Valentine and Moss, 1997) and acoustic orienting (see Fig. 1*B*,*C*) (Shimozawa et al., 1984; Covey et al., 1987; Casseday et al., 1989). On the motor side, microstimulation in the SC of *Eptesicus fuscus* can trigger sonar call production, in addition to head and pinna movements (Valentine et al., 2002). Similar findings have been reported using microstimulation techniques in the SC of an old world bat species, *Rhinolophous rouxi* (Schuller and Radtke-Schuller, 1990). Control experiments that involved stimulation of the adjacent periaqueductal gray failed to elicit sonar calls but instead evoked signals characteristic of communication calls (Valentine et al., 2002).

Based on the widespread role of the SC in orienting and the audiomotor specializations identified in the bat SC, we investigated the functional relationship between SC neuronal activity and sonar vocal production in freely echolocating bats. To accomplish this, we developed chronic neuronal recording techniques for use in unrestrained and freely behaving bats (see Fig. 1*D*). We focused on the relationship between the temporal pa-

Received June 25, 2006; revised Oct. 26, 2006; accepted Nov. 17, 2006.

This work was supported by National Institutes of Mental Health Grant MH056366 (C.F.M.) and a National Research Service Award (S.R.S.). Additional support was provided by the Comparative and Evolutionary Biology of Hearing Training Grant DC000046-11 (S.R.S.) and a P-30 Core Grant DC004664-05 (R. J. Dooling, principle investigator). We thank Chen Chiu for collection of free-flight vocal data. Murat Aytekin, Ray Gracon, Marc Holderied, Timothy Horiuchi, Yao Li, Katrina Macleod, Edward Smith, and Nachum Ulanovsky provided valuable comments and technical assistance.

Correspondence should be addressed to Shiva Sinha at his present address: Department of Physics, Swain Hall West, Indiana University, Bloomington, IN 47405. E-mail: srsinha@indiana.edu.

DOI:10.1523/JNEUROSCI.2683-06.2007

 0270-6474/07/270098-13$15.00/0

rameters of sonar calls and SC activity and specifically set out to (1) identify whether premotor neural activity in the SC was coupled directly with sonar call production times, and (2) determine relationships between vocal premotor activity and sonar vocal parameters.

Materials and Methods

Animals

Adult insectivorous bats (*Eptesicus fuscus*) ranging from 13 to 18 g were collected from the attics of private homes in Maryland and housed in a bat vivarium at the University of Maryland, College Park. Bats were housed under constant reversed 12 h light/dark conditions and given water *ad libitum*. Bats were maintained at ~80% *ad libitum* body weight and given food as a reward in behavioral experiments. The Institutional Animal Care and Use Committee at the University of Maryland approved all of the procedures described here.

Free-flight behavioral experiments

We recorded the sonar vocalizations produced by freely flying and foraging bats in a large flight room. These sonar vocal patterns served as a reference collection that we used for comparison with the sonar vocalizations produced by bats in our chronic neural recording experiments. *E. fuscus* were trained to capture tethered whole mealworms (*Tenebrio molitor*) in a large flight room (6.4 × 7.3 × 2.5 m) (see Fig. 2*A*) lined with Sonex acoustic foam (Acoustical Solutions, Richmond, VA). Mealworms were suspended at a height of ~1.5 m above the floor by monofilament line (0.1 mm diameter; Trilene Ultra Thin) within a 5.3 m target area in the center of the room. A mealworm was suspended at a randomly selected location within the target area, and then the bat was released in a random direction; the bat oriented by echolocation to find the tethered mealworm. Free-flight experiments were conducted under open-room conditions in which no obstacles were in the vicinity (within 1 m) of the tethered insect prey. Once each bat achieved a consistent capture rate of nearly 100% in open-room conditions (typically within 2 weeks of introduction to the task), audio and video recordings of its capture behavior began. Most trials were recorded on video using two high-speed cameras [MotionCorder (Eastman Kodak, Rochester, NY), 240 Hz; see below] that permitted 3-D reconstruction of the bat's flight path. To prevent the bat from memorizing the target location, the mealworm was suspended outside the calibrated video recording space 50% of the time, and data from those trials were not analyzed.

Echolocation signals were recorded using two ultrasonic transducers (Ultrasound Advice, London, UK) placed within the calibrated space. Microphone signals were amplified, bandpass filtered (10–99 kHz, 40 dB gain) (VBF-7; Stewart), and sampled at 240 kHz/channel using a Wavebook 512 data acquisition device (IOtech, Cleveland, OH). The Wavebook was attached to a laptop computer (Inspiron 7000; Dell Computer Company, Round Rock, TX) and recorded 8.18 s of audio (see below). The experimenter triggered the system on each trial after the insect capture was attempted and/or accomplished. An end trigger was used to record the behavior leading up to and just after insect capture trials and simultaneously stopped the audio and video acquisition.

Experiments were performed using only long-wavelength lighting [>650 nm; Plexiglas 2711; Reed Plastics (Beltsville, MD) and Bogen Filter 182] to eliminate the use of vision by the bat (Hope and Bhatnagar, 1979). Video recordings were made with two, frame-synchronized, high-speed video cameras (MotionCorder; Eastman Kodak) using 640 × 240 pixel resolution, 240 Hz frame rate, and 1/240 s shutter speed. The video buffer size permitted 1963 frames, allowing for 8.18 s of recorded data. Cameras were positioned just below the ceiling, in the corners of the flight room, and aimed toward the room center. The region of the flight space over which camera images overlapped was calibrated with a (nine-arm) calibration frame (Peak Performance Technologies, Englewood, CO) and filmed by both cameras before each recording session. The high-speed video cameras were used to record target position, bat flight path, and capture behavior. The resulting images were used in calculating the 3-D positions of the bat, target, and microphones.

Platform behavioral experiments

Two different behavioral tasks were used to engage bats in echolocation behavior while resting on a platform and permitting tethered chronic neuronal recordings. In both behavioral paradigms, sonar vocalizations were compared with sonar call parameters taken from bats engaged in free-flight insect capture experiments. In each task, vocal and neural data were digitally recorded simultaneously and stored to a computer hard disk. All recording devices were synchronously triggered using a single-trigger signal initiated by the experimenter. When video recordings were made, the trigger simultaneously controlled video acquisition.

Virtual target amplitude discrimination experiments

Past experiments have demonstrated the efficacy of virtual target simulators to engage bats in echolocation tasks as they rest on a platform. Bats use the time delay between their sonar vocalizations and returning echoes to determine the distance of an object (Hartridge, 1945; Simmons, 1973), and they accept as "echoes" delayed playbacks of their sonar vocalizations, delivered through a loudspeaker. These virtual echoes are apparently perceived as targets at a distance corresponding to the playback delay (Simmons, 1973). Such phantom targets can be electronically manipulated and exclude visual cues (Moss and Schnitzler, 1995). Given the success of this experimental method, in our first set of chronic recording experiments, we used a target simulator and trained bats to vocalize and discriminate delayed playbacks of their sonar calls that varied in amplitude.

Apparatus. Virtual target amplitude discrimination (VTAD) experiments used an apparatus that recorded, digitized, electronically delayed, and played back to the bat sonar signals that simulated echoes from targets. Bats were trained to rest on an elevated platform and produce sonar vocalizations. A horizontally oriented condenser microphone (Ultrasound Advice) was positioned 105 cm in front of the bat and 1.0 cm below the platform height to transduce the bat's sonar vocalizations (see Fig. 2*B*,*C*). The bat's echolocation sounds were hardware filtered (20–99 kHz as a result of processing constraints), digitized, electronically delayed, attenuated, bandpass filtered (20–99 kHz), and broadcast back to the bat through a custom electrostatic loudspeaker, with a flat frequency response (±5 dB) between 25 and 100 kHz. An ultrasonic loudspeaker for playback was positioned in front of, and just above, the condenser microphone to eliminate feedback. Virtual target experiments were conducted in a double-walled acoustic booth [2.5 × 2.5 × 2.5 m; Industrial Acoustics (Bronx, NY)]. The room interior was lined with acoustic foam to minimize sound reflection. In every experiment, low-level, long-wavelength lighting (>650 nm) outside the spectral sensitivity range of this bat species was used to eliminate visual cues (Hope and Bhatnagar, 1979).

The bat's sonar calls return echoes from the microphone, speaker, and other objects in the room that the bat must separate from the electronically delayed playback signals that simulate target echoes in behavioral tasks. Steps were taken to position the microphone and speaker of the target simulator, along with other objects in the room, to minimize overlap between the bat's vocalizations, echoes from physical objects, and phantom target echoes (delayed vocalizations). In previous experiments using this system, bats learned to respond to electronically delayed sonar signals as target echoes (Wadsworth and Moss, 2000; Moss and Surlykke, 2001).

Behavioral procedure. The VTAD task required the bat to produce sonar calls while listening to attenuated, delayed sonar call playbacks. Bats were trained in a two-alternative forced-choice task to discriminate between two sets of virtual target echoes delivered through the centrally placed loudspeaker. In one set of signal playbacks, the attenuation was set to 5 dB ("loud"), and, in the alternative set of playback signals, the attenuation was set to 20 dB ("soft"). Each trial contained 20–30 bat vocalizations and their corresponding playback echoes. At the end of each trial, the playback channel was inactivated by the experimenter (removing the virtual target), and bats were required to report whether the phantom target echoes were loud by turning to the right or soft by turning to the left. Correct responses were rewarded with food (a piece of mealworm). Head aim was monitored during training, and trials were aborted if head aim deviated by >10° from the centrally placed speaker (see below).

Training continued until head movements were maintained consistently at <10° from center. To attain a consistent level of performance, 1–3 weeks of training were required for each animal, with daily sessions to maintain performance.

The amplitude of the playbacks fall in the range of behaviorally relevant echo amplitudes for bats (Moss and Schnitzler, 1995). For every vocalization the bat produced, it received an electronically delayed signal playback that varied between 1 and 5 ms. The electronic delay adds to the acoustic travel time of the sonar signal from the bat to the microphone and from the loudspeaker back to the bat (~6 ms), yielding a total echo delay between 7 and 12 ms. This range of delays is also behaviorally relevant to the echolocating bat and corresponding to target distances between 1.2 and 2.1 m. Sonar vocalizations and virtual target echoes were visually monitored on a digital oscilloscope during sessions. Given the directional sensitivity of the microphones used and the threshold for triggering of the echo playback system, head aim that deviated by more than ~10° failed to trigger the playback system. The experimenter monitored the oscilloscope throughout each trial. If bats were vocalizing off axis from the microphone, trials were aborted.

On a subset of virtual target discrimination trials, high-speed video recordings of head and pinna movements were taken. An infrared-sensitive high-speed video camera was mounted 0.5 m above the bat with a zoom lens to record close-ups of head and pinna movements in the horizontal plane. Video recordings were made of infrared reflective markers positioned on the bat's head (two markers), body (two markers), and pinna (two markers on each external ear) while the bat performed in the echo playback discrimination task. The reflective markers were easily distinguished from background in video images. Video data were recorded at 250 Hz (1 frame/4 ms), and the video buffer permitted acquisition of 9 s of data that was downloaded to digital videotape for off-line analyses. Because of the limitations of our data storage device, video recordings were only made of a subset of trials in a session.

Behavioral analysis. All sonar vocalizations were analyzed using custom sound analysis software written in Matlab (MathWorks, Natick, MA). The start and end frequencies, duration, bandwidth, repetition rate, and pulse interval (PI) of the fundamental component of the bat's frequency-modulated (FM) sonar calls were manually marked for measurement. On trials in which video recordings were made of the head and pinna, trial segments were identified in which all markers were clearly visible and the bat vocalized. For these segments, all six markers were manually digitized in a time window around (±80 ms) the sonar vocal onset. Data were analyzed using custom software written using Matlab was used. Three measures were calculated from the video marker data: angular rotation position, angular velocity, and angular acceleration, all relative to the body. The data were smoothed using an eight-point sliding window average, to eliminate video marker tracking errors introduced by the manual marking procedure. These video data segments were analyzed to determine possible temporal relationships between sonar calls and ear or head movements. For each measure, to allow across-session comparisons, measures derived from the video segments were normalized by calculating the statistical *Z*-score at each time instance in the peri-vocal time window. Other time spans (±60 and ±100 ms) around sonar vocal onsets were also tested but showed no qualitative difference from the ±80 ms window. Trials with periods of vocal inactivity and abortive movements were examined but excluded from summary records.

Real oscillating target tracking experiments

The duration, repetition rate, and bandwidth of sonar vocalizations in virtual target amplitude discrimination experiments is limited, and vocal signals lack the temporal dynamics observed in natural field settings or in the laboratory flight room (Surlykke and Moss, 2000). To evoke the more dynamic and adaptive sonar call patterns characteristic of a foraging bat, we introduced a second task with a real moving target to more thoroughly examine the relationships between sonar vocal production and SC neural activity.

Apparatus. In the real oscillating target tracking (ROTT) paradigm, bats were trained to rest on an elevated platform (95 cm) and use echolocation to track and capture a moving edible target (see Fig. 2*D*). Mealworms (*T. molitor*), used as the edible targets, were pierced with a sewing needle and held loosely tethered on a 0.2-mm-diameter, 5-cm-long nylon line. The nylon line was hooked at one end and attached to the sewing needle. The needle was attached to a small-diameter (0.3 cm) 54-cm-long steel arm, connected to a vertically hanging pendulum arm (170 cm) (see Fig. 2*D*). This arrangement ensured that the needle was held securely on the arm, but the nylon line could easily be dislodged if the bat pulled on the target. The target moved along an arc, and the platform position was adjusted to ensure that the target intersected the bat's position on the platform. Only at this position was the bat able to capture the food reward. Neural data were continuously recorded during the session. Vocal data were recorded in 10 s blocks around the target oscillation time, and each block constituted a trial. Fifteen to 30 trials were run for each recording session.

Target position relative to the bat was determined using two condenser microphones (Ultrasound Advice). One microphone remained stationary, ~250 cm in front of the bat and 40 cm above the ground, referred to as the floor microphone. The second microphone, referred to as the pendulum microphone, was mounted on the swinging pendulum arm, 10 cm behind the target and 30 cm to the side of the target (see Fig. 2*D*) and oriented toward the platform. Both microphone signals were simultaneously recorded with a National Instruments (Austin, TX) 6110 data acquisition card at 500 kHz/channel, using custom software written in the C programming language.

Sonar signal analysis. Sonar vocalizations were quantified for each trial with custom sound analysis software written in Matlab. Trials with periods of vocal inactivity and abortive movements were examined but excluded from summary records. Off-line analysis of vocalizations was performed on the data from the stationary floor microphone. The data were filtered (10–100 kHz), rectified, and convolved with a square window (0.5 ms). Events that exceeded a set threshold were identified as sonar calls. The threshold was established as 5× the SD above the mean background level during a quiet period. Threshold crossings were used to calculate the onset and offset time, duration, repetition rate, and pulse interval of sonar vocalizations within each trial. The recorded vocal signals from the floor microphone were analyzed to determine the start and end frequencies of signals produced by the bat in a subset of trials.

Target position calculation. Vocal signals from the two microphone channels were filtered (10–100 kHz) and cross-correlated. The time lag at the maximum peak in the cross-correlation was used to estimate the separation distance between the two microphones. Calibration measurements were taken of the microphone and pendulum positions before and after each recording session. These measurements were used to determine the range of angles the pendulum moved through and the distance to the platform at each point in its swing. From this information and the time delay between the microphones when a vocalization was recorded, the distance between the target and bat was calculated.

Neurophysiology

Surgery. Bats were anesthetized with isoflurane gas (2–3%, 700 cc/min O_2; NLS Animal Health, Owings Mills, MD). The muscles of mastication overlying the skull were deflected from the midline exposing the skull surface. A stainless steel self-tapping bone screw (Fine Science Tools, Foster City, CA), inserted rostral to the cortex over the olfactory bulb region and was then secured for use as an animal ground. A craniotomy was performed over one SC exposing the dura mater. The SC is on the dorsal surface of the brain (Fig. 1*C*) and well identified using skull landmarks (Valentine and Moss, 1997). A custom, light-weight (<0.5 g), 16-channel electrode interface board (EIB) (Neuralynx, Tuscon, AZ) was positioned over the craniotomy site. The implant was constructed of four to nine, 30-gauge stainless steel cannula, soldered in a 3 × 3 matrix configuration to the EIB, with the cannula tips angled (20°) toward the central cannula. Adjacent electrodes were spaced 350 μm apart at the level of the EIB board. The EIB was a printed circuit board with no electronics and with a 20-pin Omnetics connector (Omnetics Connector, Minneapolis, MN) for mating during experiments to an active headstage board. The cannulas served as extra-cranial guide tubes and functioned as a means of electrical contact between the electrodes and the EIB. Generally, three to seven cannulas were loaded with 75-μm-diameter

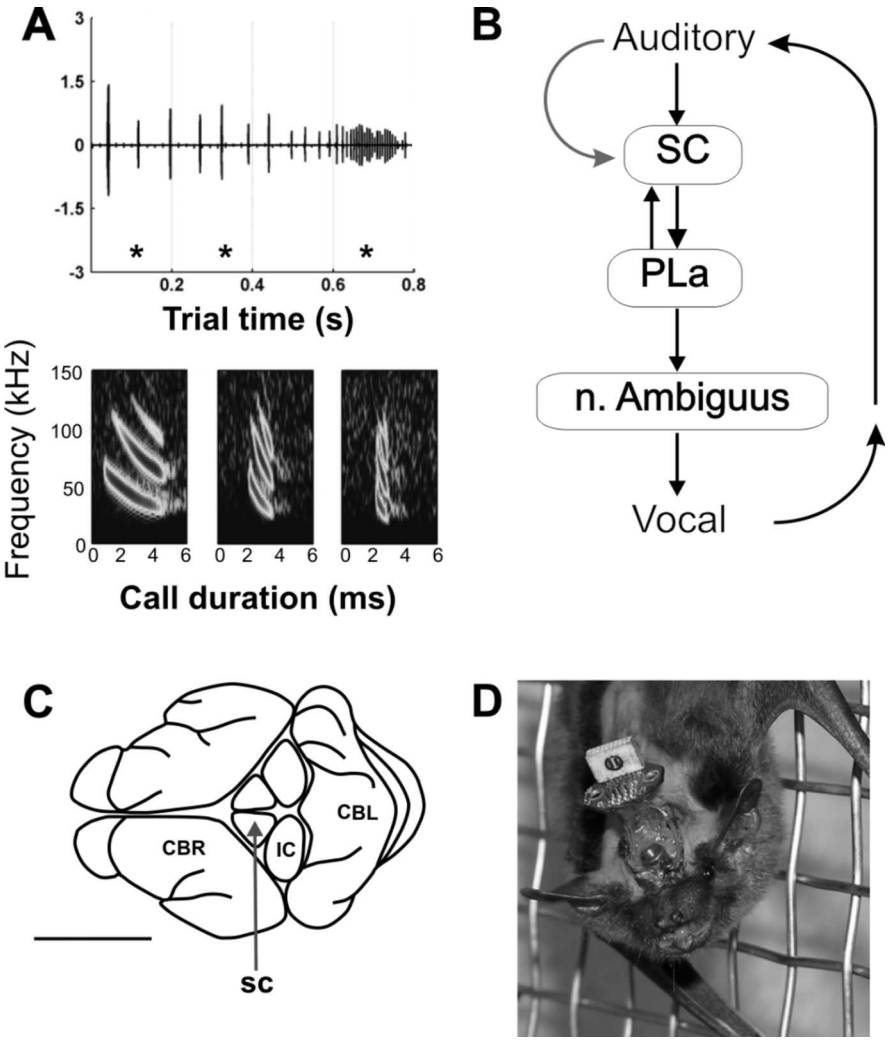

Figure 1. Sonar vocal behavior, audiovocal neuronal circuitry, dorsal SC position, and experimental subject. ***A***, Time waveform and selected spectrograms of a sequence of sonar vocalizations produced by a flying bat attacking a stationary insect target. Typical of an insect pursuit sequence, there are dynamic changes in the sonar pulse intervals as bats approach and capture a target (top). The representative spectrograms demonstrate the change in bandwidth, call duration, and sweep rate during insect capture (bottom). Asterisks are positioned below calls for which spectrograms are shown. ***B***, Network of input–output pathways that connect the SC with the sonar vocal production circuitry. Lemniscal (black arrow, top) and paralemniscal (gray arrow, at side) auditory inputs are integrated in the SC, which in turn projects to the laryngeal motor neurons indirectly via a tecto-tegemento-bulbar pathway. ***C***, Top view drawing of the bat brain showing the dorsomedial position and relative size of the superior colliculus compared with adjacent structures. CBR, Cerebrum; CBL, cerebellum. Scale bar, 5 mm. ***D***, Photograph of a 15 g bat with chronic implant before recording session. The small interface board mates with a removable amplifier head-stage board.

platinum–iridium wire recording electrodes (1.0–3.0 MΩ; Microprobe, Bethesda, MD). A single cannula was loaded with a 1.0 kΩ platinum–iridium reference electrode. The EIB was positioned with a three-stage micromanipulator over the craniotomy site, and the exposed dura was covered with biomedical grade SILASTIC (Dow Corning, Corning, NY). This prevented cynoacrylate, used to secure the implant, from contacting the brain. The EIB was attached to the skull with medical-grade cynoacrylate (Loctite 4113; Loctite, Hartford, CT). A fine insulated, 32-gauge wire attached to the bone screw was then secured to the implant and served as animal ground. The inferior colliculus (IC) in this bat species is located immediately caudal to the SC on the dorsal surface (Fig. 1*C*). In cases in which IC neural recordings were made, the craniotomy was centered ~500 μm lateral to and 500 μm posterior to the caudal SC, and the same procedure as described for SC recordings was performed.

Neural data collection. Bats were allowed to recover for several days after surgery before being returned to the behavioral apparatus for experimental testing and neural recording. On recording days, a head-stage board (20 × 10 mm; <1 g) (HS-16M; Neuralynx) with unity-gain buffers was connected to the implanted EIB. A lightweight, 38-gauge wire tether transmitted data from a maximum of 16 neural channels to a Cheetah 32 Digital Interface data acquisition system (Neuralynx). After amplification (5000–10,000×) and bandpass filtering (0.100–6 kHz), neural activity was recorded continuously, along with synchronization signals from the Neuralynx system. Electrodes were advanced by 75–100 μm between recording sessions and at least 12 h before the start of each recording session. A new site was studied in each recording session, lasting 30–50 min, during which time the bats remained connected to the recording system. Movement of the bats was not encumbered by the head-stage and tether assembly because they vocalized freely and performed at ≥80% success rate in echolocation tasks. After each session, data were archived to compact disks and analyzed off-line.

Neural data analysis. All off-line analyses were performed using custom software written in Matlab. The continuously recorded wide-band extracellular potentials were first digitally band-pass filtered (0.3–6 kHz). To extract the times of neural events, the following procedure was followed. The power (root mean square) of the entire filtered signal was computed in a sliding square window (0.25 ms) for neural event detection (Bankman et al., 1993). The overall SD was calculated to estimate the variance of the baseline activity and to establish a neural event detection threshold. Potential neural events were identified in regions in which the power of the continuously sampled voltage records was 2 SDs greater than the overall mean power level. From these potential neural events, only those events that met the following criteria were accepted: (1) the power remained above threshold for <3.0 ms, (2) the power remained above threshold for a minimum of 0.5 ms, (3) neural events were separated by a minimum of 0.5 ms, and (4) the waveform shape corresponded to a positive voltage deflection, followed by a negative voltage deflection. This subset of events was treated as "spiking" events for additional analysis. There was no evidence from the extracellular potential waveforms that we were recording fibers of passage, and the low electrode impedances make it unlikely that fiber activity was dominant. The consistent pattern of neural activity, across all recording sites, also makes it unlikely that recordings were from fibers of passage.

To determine whether the pattern of neural activity before sonar vocalizations substantially differed from the background event rate, we used the following method. First, a background neural event rate was established from a 1-s-long, nonvocalizing period, preceding the start of a session and the start of randomly selected behavioral trials. Second, neural and vocal data were aligned, referenced to a common sync signal. Third, time windows around each sonar vocal onset time in a trial were identified in the neural data, segmented out, and aligned using vocal onset time. Raster plots and perimotor time histograms (PMTHs) were constructed from this vocal onset aligned neural data. For VTAD experimental trials, pulse intervals were large (>80 ms). Therefore, a time window extending 60 ms before to 10 ms after sonar vocal onset was used. A similar time window was used for ROTT trials. However, ROTT trials (and some VTAD trials) included calls with shorter pulse intervals (<80 ms). Consequently, for calls with shorter pulse intervals, a time

window the length of the pulse interval was used in analyses. Time windows for consecutive calls were never overlapping. PMTHs were constructed with 1 and 2 ms bin widths. No difference in the PMTH pattern was observed using different time bins, so 2 ms bins were subsequently used. Bins were identified in which the number of neural events exceeded an event threshold. This threshold was set at a level of 2 SD above the mean background event rate. Other event threshold levels were tested (1 and 3 SD) but produced little change in the calculated occurrence of neural events. Events in bins that exceeded this event threshold were used for subsequent analyses. Neural events were distributed bimodally in rasters and PMTHs (see Fig. 6*A*, bottom). The mode with longer lead times comprises long lead events (LLEs) and is referred to as the LLE bout. The mode with shorter lead times comprises short lead events (SLEs) and is referred to as the SLE bout. The following measures were used to quantify LLEs and SLEs: the across-trial mean time of LLE or SLE, the mean time of LLE before each sonar call, $\langle \mathrm{LLE} \rangle_{\mathrm{TIME}}$, the SD ($\pm 1$) of LLE preceding each call, $\langle \mathrm{LLE} \rangle_{\mathrm{SPREAD}}$, and the firing rate of LLE preceding each sonar call, $\langle \mathrm{LLE} \rangle_{\mathrm{FR}}$. For $\langle \mathrm{LLE} \rangle_{\mathrm{FR}}$ calculations, events in over-threshold bins, within the time interval of the LLE bout, were used for the calculation.

Histology. Bats were deeply anesthetized with sodium pentobarbital (0.04 ml/bat, i.p.). Intracardial perfusion with saline was followed by a 4% buffered paraformaldehyde fixative, and the brain tissue was removed from the skull and blocked. The brains were subsequently stored in sodium PBS (0.1 M), pH 7.2, with 30% sucrose overnight, sectioned at 40 μm on a sliding freezing microtome, mounted and Nissl stained. Electrode tracts were reconstructed based on this material.

EMG recordings. Teflon-coated silver wires (0.12 mm diameter; Medwire, New York, NY) were threaded through 30-gauge hypodermic needles, with the ends fashioned into hooks, which protruded from the sharp ends of the needles. Pairs of wires were inserted close together into the muscles of mastication. The wires were placed so that they were close to the SC and above the midsagittal sinus. The wires were secured in place using tissue adhesive, and the protruding exposed ends of the wires were soldered to gold pins. When recording EMG activity, the gold pins were connected to a DAM 80 amplifier (World Precision Instruments, Sarasota, FL), filtered (1–3000 Hz), and amplified (5000×), and the data were recorded to computer via a National Instruments PCI6110 data acquisition card for later analysis. Vocal signals were recorded using an Ultrasound Advice condenser microphone, filtered (10–99 kHz), amplified (2–5×), and simultaneously recorded with the EMG data on a separate channel of the National Instruments card. The data acquisition card sampled each channel at 300 kHz. Vocalizations were analyzed as described for platform experiments. EMG data were analyzed in the same manner as SC neural data.

Results

Sonar vocal behavior

We recorded sonar vocal sequences produced by echolocating bats during free-flight insect capture trials in a large laboratory flight room. These sequences served as the reference dataset for sonar calls produced in the chronic neural recording behavioral trials and were used to determine whether our platform behavioral experiments evoked naturalistic sonar production patterns. Insectivorous bats of the species *Eptesicus fuscus* produce FM sonar vocalizations with dynamic signal features that depend on target location in azimuth, elevation, and distance. In field recordings, both call duration and PI (time between onsets of consecutive calls) vary with target position. These characteristic changes are commonly used to divide insect pursuit into different stages, search, approach, and attack (Griffin, 1958; Simmons and Kick, 1984; Surlykke and Moss, 2000) (Table 1), and are observed in our flight room trials. When free-flying bats attack stationary tethered mealworms in the flight room (6.4 × 7.3 × 2.5 m) (Fig. 2*A*), the variation in sonar features is strongly related to target distance (Fig. 3*A*, left column, 14 separate free-flight attack sequence trials recorded from four different bats). The flight path and sonar call features used by the bat are representative of the bat's natural insect capture behavior. The flight room primarily restricts the range of vocalization features produced by the bat, mostly by constraining the duration of search calls to 5–6 ms, because bats avoid overlap between its sonar cries and returning echoes from the floor, ceiling, and walls. The plot shows a monotonic decrease in sonar call duration with target distance. Generally, bats in the laboratory flight room do not fly directly toward insect prey but instead display a curved intercept flight path. This curved flight path may account for the scatter observed in the relationship between call duration and target distance. For the largest PIs (>100 ms), associated with the search phase, there is only a weak relationship between call intervals and target distance. The approach phase is marked by a consistent decrease in call duration (8 down to 2 ms) and PI (100–20 ms) with decreasing target distance. The attack phase begins when the bat is <1 m from its prey and is characterized by the shortest sonar calls (<1 ms) and short PIs (<10 ms). Overall, sonar call duration decreased linearly and the PI decreased in a piecewise exponential manner, when the bats approached a stationary target in free flight.

Table 1. Foraging bats adjust the features of sonar vocalizations as they search for, approach, and intercept a target

Insect pursuit phase	Sonar call rate (Hz)	Sonar call duration (ms)
Search	5–10	15–20
Approach	20–80	2–5
Terminal buzz	0.5–1.0	150–200

The characteristics of their sonar vocalizations have been used to divide this bat's insect pursuit vocal sequence into three different phases (Griffin et al., 1960).

In contrast to the dynamic pattern of echolocation calls produced by the bat when it engages in free-flight insect capture, the range of the sonar vocalization parameters produced by the bat was more restricted in the virtual target discrimination condition (Fig. 3*B*). The data come from two animals, recorded over 30 trials, with trial lengths varying from 6 to 20 s. The sonar call durations recorded from animals engaged in the virtual target discrimination condition did not change over trial time and were limited primarily to 3–4 ms (Fig. 3*B*, top); thus, animals performing in this task do not produce very short or long duration calls, nor do they modulate the signal repetition rate with changing playback parameters (Fig. 3*B*, bottom). The PIs in this virtual target discrimination experiment were an order of magnitude greater than in free-flight trials. No discernable patterns of variation in the sonar call duration and PI were observed during virtual target discrimination trials, and no overall pattern was observed across trials.

The vocal behavior of the bat engaged in the ROTT experiments (Fig. 3*C*) showed important similarities and differences from those observed in the free-flight insect capture trials. Similar to the free-flight case, the bat's sonar call duration in the oscillating target experiment decreased steadily with target distance, and it spanned similar call durations over the range of target distances studied (0.0–1.6 m). In contrast to the free-flight case, the rate of change of the bat's call duration with target distance was smaller (Fig. 3*C*, top). The relationship between sonar call PIs and target distance in the ROTT experiments was exponential, similar to the free-flight case, across a wide range of target distances investigated (Fig. 3*C*, bottom), but the PIs produced by the bat spanned a 5× larger range of values in the oscillating target task compared with those recorded in the free-flight experiments. The extended interval of short PIs produced by bats at short target distances in the free-flight case was not evident in the oscillating target trials, except at the very shortest distances (<0.2 m), although the bat used a similar range of short PIs.

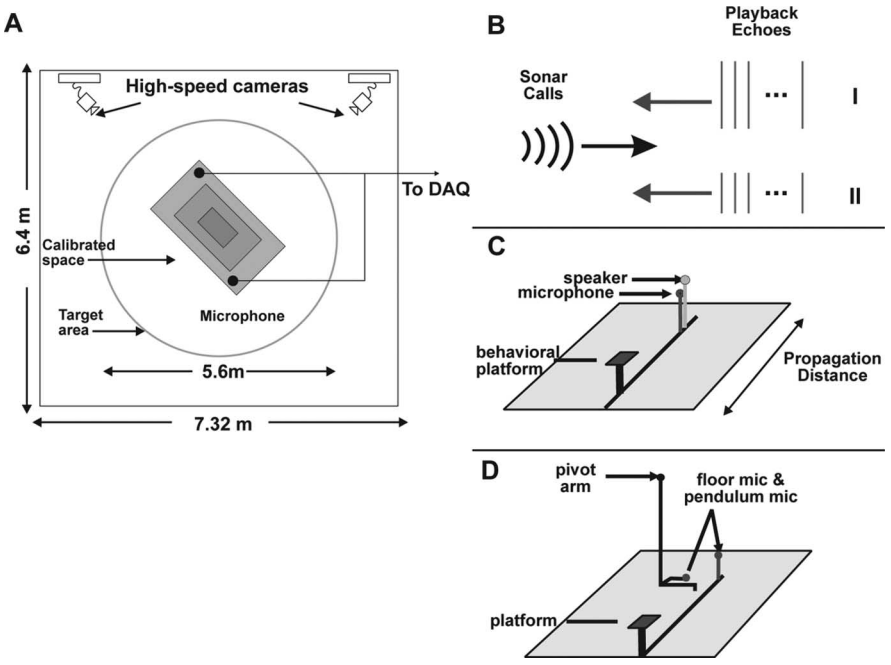

Figure 2. Experimental design for the flight room experiments and the two different behavioral paradigms used for chronic recordings. ***A***, Top view of the flight room, showing position of high-speed cameras (240 frames/s). Bats are permitted to fly within the entire room, but the edible target is only hung within the target area. ***B***, During virtual target amplitude discrimination trial sonar calls produced by a bat are acquired, modified to simulate sonar echoes, and played back to the bat. Playback echoes are either from a loud intensity group (I) or a soft intensity group (II). The delays of the playback echoes are randomly chosen during the trial from a limited range of values (7–12 ms). ***C***, Schematic of the virtual target amplitude discrimination setup. Bats rest on a behavioral platform and produce sonar vocalizations directed toward an ultrasonic microphone. The signals are modified by a computer and played back to the bat via a speaker positioned above and behind the microphone. ***D***, Schematic of the real oscillating target tracking setup. Bats are trained to rest on a platform and use echolocation to track and capture a moving target. The target, positioned on a horizontal arm connected to a single pivot point vertical pendulum, swings in a single plane intersecting the bat's position.

Representative data from one oscillating target trial (Fig. 4*A*) shows changes in the bat's call duration as a function of target distance over the course of a single trial and demonstrates the changes in vocal call duration and PI used when the bat tracked the moving target. In the beginning of the trial, the target was held at the start position and the bat consistently used longer duration calls. When the target was released, the bat steadily decreased the duration of the sonar cries it produced, called only a few times when the target receded, and again used a sequence of decreasing call durations during the second approach. This variation in call duration is exponentially related to changes in PI (Fig. 4*B*), evident in the log-linear plot, and both parameters covary with target distance. Thus, the dynamic target-oriented vocal behavior observed during the oscillating target paradigm resembled the vocal behavior observed during free-flight insect capture.

In contrast, the bat's vocal behavior during the virtual target discrimination paradigm does not show the dynamic variation in call parameters as seen in the free-flight case. Instead, the bat's call parameters were more similar to those produced by the bat when it was at greater distances relative to the target, and it may have been still searching for the target. Note that the range of echo delays in the virtual target discrimination experiment was 6–12 ms, corresponding to target distances of ~1.1–2.1 m.

Premotor activity in the superior colliculus

Virtual target amplitude discrimination

In our first set of chronic recording experiments, we wanted bats to freely and consistently produce sonar vocalizations. Therefore, bats in VTAD experiments were trained to spontaneously vocalize. For each sonar vocalization produced, they were presented with an attenuated, delayed playback of that sonar call (see Materials and Methods). Bats emitted species-specific downward-sweeping, multi-harmonic, short-duration (2–4 ms) sonar vocalizations when performing this echo amplitude discrimination task (for sample sonar vocalization, see Fig. 5*A*). Neural activity recorded in the SC during this task was characterized by a low mean baseline event rate (20 ± 17 events/s; $n = 10$ sites, 2 bats). In addition, preceding the onset of sonar vocalizations, a regular increase in neural activity was observed (Fig. 5*B*). An exemplar extracellular voltage trace for a 5-s-long segment (Fig. 5*B*) shows peaks in premotor activity coinciding with sonar call onsets (red, vertical ticks). This temporal coincidence is more evident in Figure 5*C*, which shows a rectified, smoothed (eighth-order Butterworth filter), and low-pass filtered (<100 Hz) version of the data from Figure 5*B* and demonstrates the close temporal correspondence between the SC neural activity and the sonar vocal onsets.

A representative raster plot and PMTH from a single virtual target amplitude discrimination trial is shown in Figure 6*A*. The plots were constructed by aligning the neural events around each sonar vocalization relative to sonar call onsets ($t = 0$ s). Each line in the raster plot displays neural activity surrounding one of the consecutive sonar calls during the trial. The premotor activity was characterized by two brief bouts of increased activity that were comprised of LLEs and SLEs, separated by a brief return to near baseline event rates. The sequence of sonar calls ($n = 68$ calls) produced during this 12-s-long trial had large PIs (> 60 ms) and durations spanning ~2–4 ms (Fig. 6*B*). The bimodal distribution in event lead times prompted us to evaluate the two groups of neural events separately. The plots in Figure 6*A* illustrate the increase in event rate preceding call onsets, the distinct reduction in event rate between LLEs and SLEs, and the return to baseline event rates before or shortly after call onset, which is evident at all of our recording sites ($n = 44$). Relative to the SLEs, the LLEs occur over a larger range of lead times (−40.6 to −8.4 ms; 10th to 90th percentile) and have a mean lead time across all trials of −22.2 ± 3.9 ms (mean ± SD; $n = 10$ sites, 2277 calls, 2 bats). The SLEs, in contrast, had a smaller range of lead times (−5.1 to −2.2 ms; 10th to 90th percentile) and an across-trial mean lead time of −3.6 ± 0.7 ms that was tightly coupled (small SD) to the call onsets ($n = 10$ sites, 2277 calls, 2 bats). Based on our threshold criterion, these events occurred consistently (>90%) before sonar vocalizations (Table 2).

To investigate whether a relationship between LLEs and sonar vocal parameters was present, three measures were used to quantitatively characterize the LLE premotor activity per call: the mean time of LLEs ($\langle LLE \rangle_{TIME}$), the ±1 SD of LLE times ($\langle LLE \rangle_{SPREAD}$), and the LLE firing rate ($\langle LLE \rangle_{FR}$) (see Materials and Methods). Additionally, to assess whether a relationship exists

between these measures and sonar call temporal features, simple one-parameter linear regression analyses were conducted between each of the three measures of LLE activity and the corresponding call durations (n = 1026 calls, from 14 VTAD trials) (Fig. 6*C*,*D*). In relation to call duration, both $\langle LLE \rangle_{TIME}$ and spread in LLE time had linear regression slopes significantly different from zero ($\langle LLE \rangle_{TIME}$, $F_{(1,1026)} = 18.0$, $p < 0.001$; $\langle LLE \rangle_{SPREAD}$, $F_{(1,1026)} = 19.5$, $p < 0.001$; F score and significance level); however, they accounted for little of the overall variance ($r = 0.014$ for $\langle LLE \rangle_{TIME}$; $r = 0.013$ for $\langle LLE \rangle_{SPREAD}$). $\langle LLE \rangle_{FR}$ had a nonsignificant slope in relation to call duration. $\langle LLE \rangle_{TIME}$, $\langle LLE \rangle_{SPREAD}$, and $\langle LLE \rangle_{FR}$ showed no significant relationship to PI.

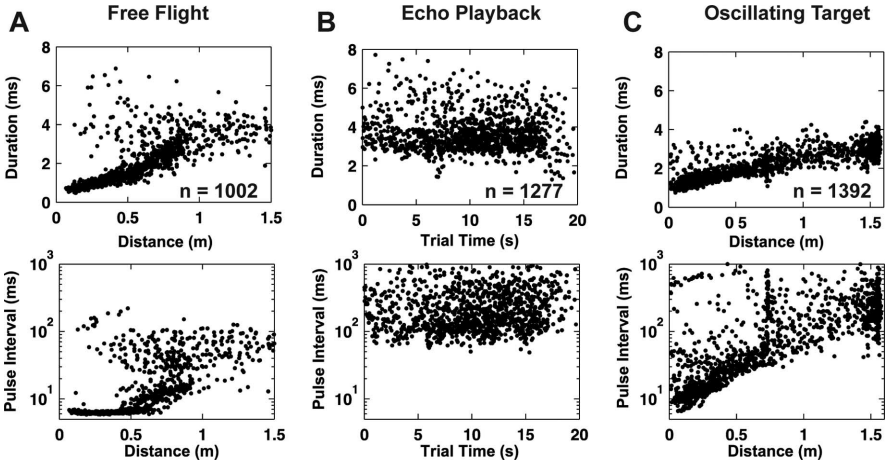

Figure 3. The temporal characteristics of sonar vocal sequences in different behavioral tasks. The sonar call duration (top row) and pulse interval (bottom row) are shown as a function of target distance or trial time. ***A***, Data from two free-flying bats attacking a stationary edible target. Sonar call duration and pulse interval show distinctive changes as a function of target distance. ***B***, During a virtual target amplitude discrimination experiment, call duration and pulse interval are large compared with the other tasks and vary in a nonpatterned manner over the course of each trial. ***C***, In real oscillating target tracking trials, bats remain stationary and a target oscillates toward and away from the bat. Sonar call duration and pulse interval vary closely with target distance. Data in ***A–C*** comprise sonar calls, from all trials, during one session. The total number of call parameters plotted for each behavioral task is shown in the top row.

Real oscillating target tracking

Bats trained in the ROTT paradigm produced sonar calls and pursuit and capture sequences similar to those recorded from bats engaged in free flight (Figs. 3*C*, 4*A*). This permitted the investigation of changes in premotor activity from the SC of a chronically implanted tethered bat producing echolocation calls characteristic of a free-flying foraging bat. A representative example of the premotor activity pattern during a single ROTT trial is shown in Figure 7. As in the VTAD experiments, we observed distinct LLE and SLE activity relative to sonar call onsets (t = 0 ms) and the return to baseline levels after call onset (Fig. 7*A*).

Neuronal activity during ROTT trials was characterized by a low mean baseline event rate (23 ± 16 events/s; n = 35 sites, 3 bats), similar to that observed in echo playback trials. LLEs occurred over a range of lead times (−29.8 to −7.1 ms; 10th to 90th percentile) and had an across-trial mean lead time of −17.5 ± 9.1 ms (mean ± SD; n = 35 sites, 15724 calls, 3 bats). For ROTT trials, the SLEs had lead times that spanned (−3.0 to +0.4 ms; 10th to 90th percentile), had an across-trial mean lead time of −1.2 ± 1.3 ms, and, as in VTAD trials, had consistently short lead times relative to call onsets (n = 35 sites, 15724 calls, 3 bats). The LLEs and SLEs occur consistently before sonar vocal onsets but with a lower incidence than in VTAD trials (Table 2). This may be attributable to the bat's much higher vocal production rates in the ROTT task.

In contrast to the consistently long pulse intervals (>60 ms) observed during virtual target amplitude discrimination experiments, bats regularly produced shorter PIs during real oscillating target tracking trials. This raised the possibility of incorrectly interpreting neural events as premotor activity instead of as potential auditory-related activity. This possibility, however, was excluded on additional evaluation. All trials from a session were segmented according to five PI groups (>50, 25–50, 16.7–25, 12.5–16.7, 10–12.5, and 8–10 ms). For each call, an associated target distance was measured, which allowed the calculation of echo arrival time. Within each PI group, neural events were aligned to echo arrival time, and raster plots and PMTHs were constructed. A range of auditory response latencies were assumed based on latencies in neurophysiological experiments (4–20 ms) (Valentine and Moss, 1997), and neural event tuning within this range was measured. No echo-evoked activity was identified under these conditions, only premotor activity associated with sonar call onsets.

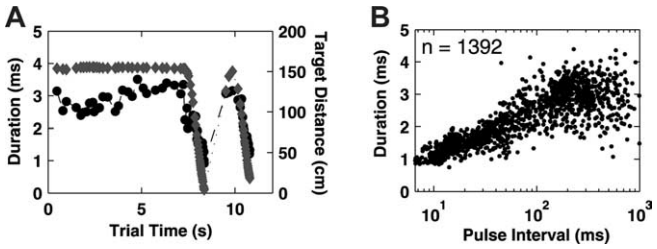

Figure 4. Variation in sonar call durations with target distance and pulse interval in a real oscillating target tracking trial. ***A***, The close coupling between sonar call duration and target distance is highlighted in an oscillating target trial. Target distance (gray diamonds) and call durations (black circles) are shown as a function of trial time (0–12 s). ***B***, Sonar call duration versus pulse interval for all 1392 calls in Figure 3*C*. Pulse interval varies over a wide range during both real oscillating target tracking and free-flight trial conditions. The exponential relationship between call duration and PI is made clear in this semi-log plot.

An interesting feature evident in ROTT raster plots is the noticeable decrease in the LLEs time over the course of the trial (Fig. 7*A*). When evaluated with respect to target distance, the decreasing LLE times occurred when the oscillating target was swinging toward the bat, i.e., approaching the bat. Based on this observation, the $\langle LLE \rangle_{TIME}$ from all trials at this recording site were calculated and plotted against their corresponding call duration (n = 1231 calls, 31 trials) (Fig. 7*C*). A clear trend was observed in which larger $\langle LLE \rangle_{TIME}$ corresponded with longer call duration, and shorter $\langle LLE \rangle_{TIME}$ corresponded with shorter call durations. A linear regression fit of these data accounted for a large fraction of the variance ($r = 0.73$) and showed a significant relationship between $\langle LLE \rangle_{TIME}$ and call duration ($F_{(1,1231)} = 1425$; $p < 0.001$). To address the possibility that LLE times were associated with the call duration of a sonar pulse later in the vocal sequence, a linear regression analysis was performed by calculating the $\langle LLE \rangle_{TIME}$ with respect to calls n calls forward in the sonar pulse sequence (n = 1, 3, 5). Using a linear regression analysis the regression coefficients steadily diminished (r = 0.57, 0.30, and

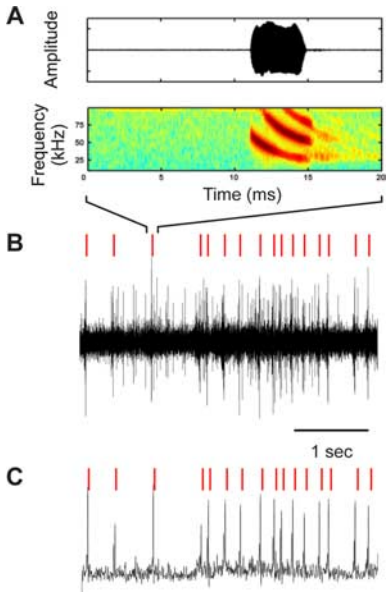

Figure 5. Premotor neural activity in the SC associated with sonar call production. ***A***, Time waveform and spectrogram of a single 3.8-ms-duration sonar vocalization produced during virtual target amplitude discrimination experiment. ***B***, Neural activity recorded simultaneously with sonar vocalizations in the SC. Bouts of neural activity in the superior colliculus consistently precede the onset of sonar vocalizations. Red ticks above neural activity in ***B*** and ***C*** are identically placed and correspond with the onset time of sonar vocalizations. ***C***, Rectified waveform of the neural activity in ***B***, low-pass filtered (<100 Hz) with an eighth-order Butterworth filter.

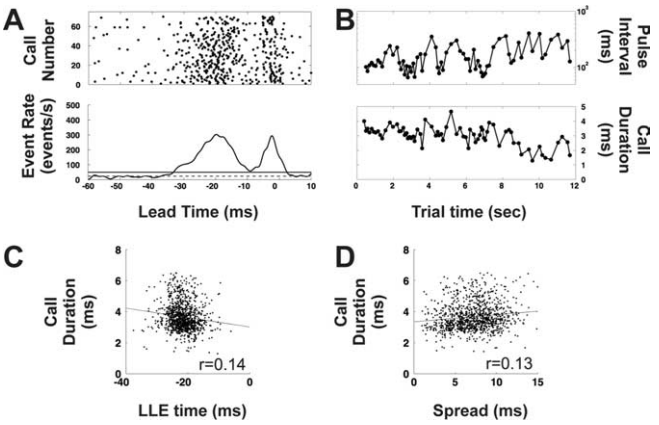

Figure 6. Sonar-related premotor activity is consistently observed in all recordings from SC. ***A***, Raster of events (top) preceding the onset of sonar vocalizations during one trial (bat VTAD1). Ordinate represents consecutive sonar calls from first to last in the trial. Call onset is at $t = 0$ ms, and the raster extends from 60 ms before to 10 ms after sonar vocal onset. During this trial, 74 sonar calls were produced, and both long and short lead events were evident. A PMTH (bottom) representation of neural events. The dashed line shows the baseline activity level, and the solid line represents the criterion threshold (2 SD above mean baseline rate) used for determining change from baseline activity. A clear reduction in firing rate is observed between the long lead and short lead events and after call onset. ***B***, The PI and sonar call duration of vocalizations produced during the trial shown in ***A***. PI is generally long, >75 ms, in virtual target amplitude discrimination trials. ***C***, Linear regression using the per call mean LLE time ($\langle LLE \rangle_{TIME}$) as the single predictor for sonar call duration. The sonar calls ($n = 1026$ calls) come from one session (including the trial in ***A***) and show only a marginal increase in $\langle LLE \rangle_{TIME}$ with increasing call duration. ***D***, Linear regression using the $\langle LLE \rangle_{SPREAD}$ (see Materials and Methods) for each call in one session as the single predictor of call duration. $\langle LLE \rangle_{SPREAD}$ shows a slight positive increase with call duration.

0.10 for 1, 3, and 5 calls forward in the vocal sequence, respectively) (Fig. 7*D*; same site shown in Fig. 7*A–C*). Similar results were obtained for each of the other 34 recording sites.

The relationship between $\langle LLE \rangle_{TIME}$ and upcoming sonar call duration was examined across all ROTT sites ($n = 35$). A linear regression analysis, performed for each site using $\langle LLE \rangle_{TIME}$ as the single predictor, showed that regression coefficients were >0.60 at most sites (23 of 35) (Fig. 8*A*). In addition, to verify that regression slopes were nonzero, a bootstrap procedure was used. For each site, 100 datasets were derived by randomly drawing (with replacement) neural event times and corresponding call durations. For each bootstrap dataset, a regression analysis was performed to determine a slope. The mean slope was then calculated for the 100 datasets, and confidence intervals were determined. In all but two cases, the bootstrap-derived mean slopes were negative, and the 95% confidence intervals did not include 0. For these 33 sites, the slopes of the linear fits (Fig. 8*B*) were in the range of (-0.03 to -0.15), with a mean ± SD of -0.084 ± 0.033. Therefore, a 1 ms increase in call duration corresponded to an ~12 ms increase in $\langle LLE \rangle_{TIME}$. An analysis using linear regression of $\langle LLE \rangle_{TIME}$ against PI accounted for <0.2 of the variance across all sites.

$\langle LLE \rangle_{FR}$ and $\langle LLE \rangle_{SPREAD}$ were also investigated in ROTT trials and related to sonar call duration. Regression analyses revealed that both of these parameters individually accounted for only a small amount of the overall variance. Combined with the $\langle LLE \rangle_{TIME}$, these three predictors marginally increased (2–15%) the overall variance accounted for, by as much as 0.14, at 19 of 35 sites when a multiple linear regression analysis was performed. The three-predictor versus single-predictor ($\langle LLE \rangle_{TIME}$) r values are shown plotted in Figure 8*C*. Single predictor linear regression analyses of $\langle LLE \rangle_{FR}$ and $\langle LLE \rangle_{SPREAD}$ against PI produced nonsignificant results.

Sonar call duration versus the SLE activity (Fig. 9) was examined in an 8 ms window (-6.0 to $+2.0$ ms) around each call onset ($t = 0$ ms) and showed no trend. This time window, across all sites, spans the above-baseline activity immediately preceding sonar call onsets. The data are taken from three different sites in three different bats, with the n values in the panels representing the number of calls that contributed to each figure ($n = 1117$, 2260, and 2268 calls). The three panels show the range of deviation we observed in our SLE data, with events occurring in a relatively small window of time before sonar onset and with fairly high precision. No obvious relationship was observed between short lead premotor activity patterns and sonar call duration or PI. Short lead events did not show any statistically significant relationship with call duration or PI when a linear regression analysis was performed, even when different event threshold levels (see Materials and Methods) were used for detecting event rates greater than the background activity rate.

Table 2. Occurrence of neural events before sonar calls for VTAD and ROTT paradigms

Behavior	Events	Occurrence	SE
Virtual target amplitude discrimination	All events	0.98	0.01
	LLE	0.98	0.00
	SLE	0.82	0.04
Real oscillating target tracking	All events	0.93	0.00
	LLE	0.68	0.02
	SLE	0.67	0.02

The neural recordings described here were made from 35 separate penetrations, at more than seven different depths in the intermediate and deep layers of the SC. We did not identify any relationships between the histologically reconstructed recording sites, in either depth or along the mediolateral or rostrocaudal

dimensions, and the pattern of premotor neural activity. The question of site specificity of the vocal premotor pattern of activity can be more thoroughly addressed with future experiments.

Controls

Four control experiments were conducted to determine whether the observed premotor activity in the SC was related to non-sonar vocalizations (i.e., communication calls), potentially to other orienting movements, or to artifacts. Data from all of the control experiments are shown in Figure 10.

First, to account for the possibility that neural activity recorded in the SC was related to all types of vocalizations (sonar and non-sonar) we made recordings while bats produced non-sonar vocalizations (Fig. 10*A*) ($n = 6$ sites total recorded). Spectrograms of the type of non-sonar calls observed here have been published in other studies (Moss, 1998; Valentine et al., 2002), but their functional role remains to be established. Raster plots (Fig. 10A, top left) and their corresponding PMTHs (Fig. 10*A*, bottom left) aligned to vocal onsets ($t = 0$ ms; spanning from 60 ms before until 10 ms after call onset) showed no distinct LLE or SLE pattern of activity. The PIs of these non-sonar vocalizations (Fig. 10*A*, top right) encompassed a similar range of PIs to the sonar vocalizations (Figs. 3*B*, 6*B*). However, these non-sonar calls had much lower start and end frequencies (within the human audible range) and a more variable range of call durations (Fig. 10*A*, bottom right). During these trials, when bats produced sonar vocalizations, premotor activity with LLEs and SLEs were consistently observed at these same sites.

Next, to account for the possibility that LLE and SLE activity could also be related to other orienting movements, high-speed video recordings (250 frames/s) were made of bats on the platform while they engaged in the echo playback experiment. Infrared markers on the pinna, head, and body were tracked for a subset of trial segments ($n = 20$ trials segments, 50 sonar calls, 3 bats). Three measures were calculated for each trial segment: angle of the head with respect to the body (θ; 0° is head–body aligned), its first derivative (angular velocity), and its second derivative (angular acceleration). Eighty-millisecond-long segments of data around each sonar call onset (±40 ms) were analyzed for each measure. Plots of these three measures did not show any consistent pattern relative to the time of sonar vocal onset. To quantitatively compare θ across trials, we normalized each trial segment by calculating a standard score and the *Z*-score and then analyzed the data. We observed a reduction in the variance of θ before the previously calculated across-trial mean LLE time (−17.5 ± 9.1 ms) for ROTT trials (Fig. 10*B*, gray bar centered on mean, with bar width representing ±1 SD). The other two measures show the expected derivative response profile. At a variable time after the sonar vocal onset, the amount of head movement increased once again. The spatial resolution of the video marker tracking procedure prevented identification of pinna movements smaller than ~1 mm. Although these small-amplitude pinna movements could have been produced, our current system cannot reliably measure them.

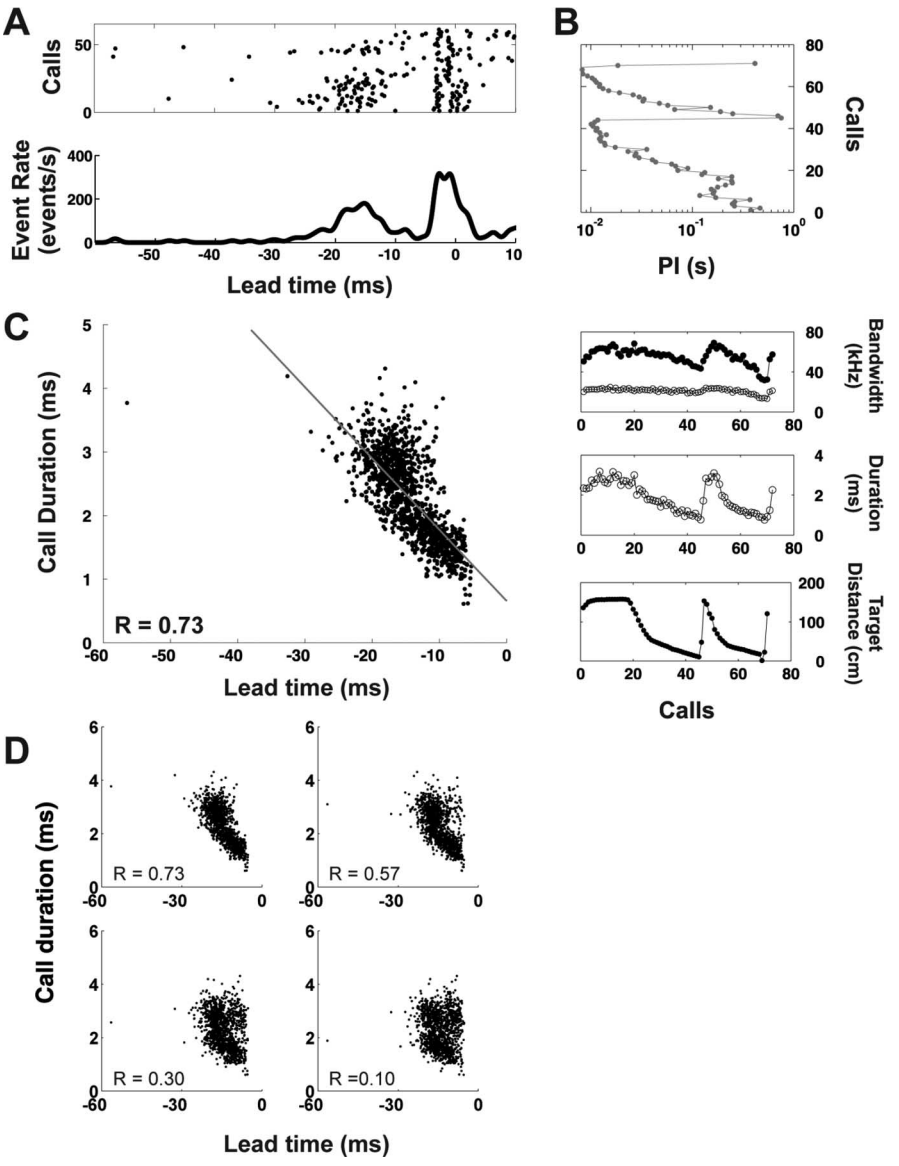

Figure 7. Premotor neuronal activity recorded in the SC during a single oscillating target trial. ***A***, Raster and perimotor time histogram show a pattern of premotor activity similar to that observed in virtual target amplitude discrimination recordings. LLEs and SLEs precede sonar vocalizations with a reduction toward baseline activity rates between the two event groups. Data are aligned to sonar call onset (lead time of $t = 0$ ms). LLEs in the raster show a tendency toward shorter lead times during the trial and correspond to times when the target is approaching the bat. ***B***, PI (gray, filled), start (black, filled), and end (black, open) frequency, call duration (black, open), and target distance (black, filled) of sonar vocalizations produced during trial shown in ***A***. The oscillating target approaches and recedes from the bat twice in this trial. Each sonar call parameter is modulated as a function of the target distance. Sonar call duration and pulse interval are clearly decreased whenever the target approaches. ***C***, Linear regression using the per call mean LLE time ($\langle LLE \rangle_{TIME}$) as the single predictor of sonar call duration for all sonar calls in one recording session ($n =$ 738 calls). The data show an increase in $\langle LLE \rangle_{TIME}$ for increasing sonar call durations ($r = 0.73$). ***D***, Reduction in the correlation between sonar call duration and $\langle LLE \rangle_{TIME}$ when $\langle LLE \rangle_{TIME}$ is not associated with the call it precedes. Each panel shows the sonar call duration versus the $\langle LLE \rangle_{TIME}$ using the data from ***C***. Except for the top left, the other panels show the data with $\langle LLE \rangle_{TIME}$ associated with the sonar call duration one, three, and five calls ahead in the vocal sequence. *r* values are regression coefficients.

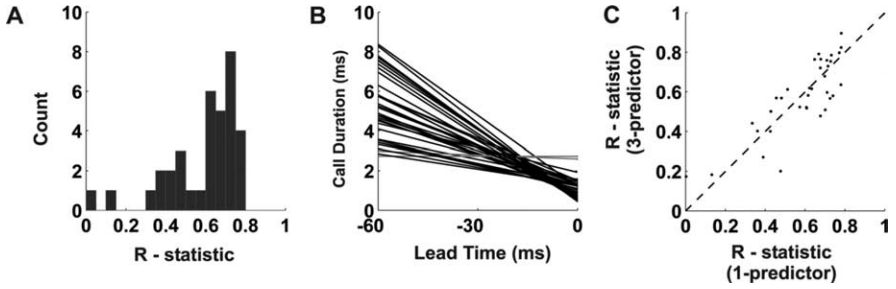

Figure 8. Linear regression analyses using per call mean LLE time ($\langle LLE \rangle_{TIME}$) to predict call duration. Linear regression analyses were performed for all sites ($n = 35$) for which sonar call duration and mean LLE time were well approximated by linear relationship. ***A***, Histogram of the *r* statistic calculated from the linear regression analyses. At each recording site, the $\langle LLE \rangle_{TIME}$ was the single predictor to estimate sonar call duration. At 23 of 35 sites, regression coefficients are >0.60. ***B***, Linear regression line fits from the 35 sites, in the superior colliculus of three bats. The mean slope for all slopes significantly greater than zero (black lines) is -0.084 ± 0.033. ***C***, *r* statistics from linear regressions using per call event rate, per call spread, and $\langle LLE \rangle_{TIME}$ as predictors of sonar call duration plotted against a single-predictor ($\langle LLE \rangle_{TIME}$) *r* statistic values. A modest increase in the magnitude of the regression coefficients is observed at the majority of sites, as demonstrated by points lying above the unity line.

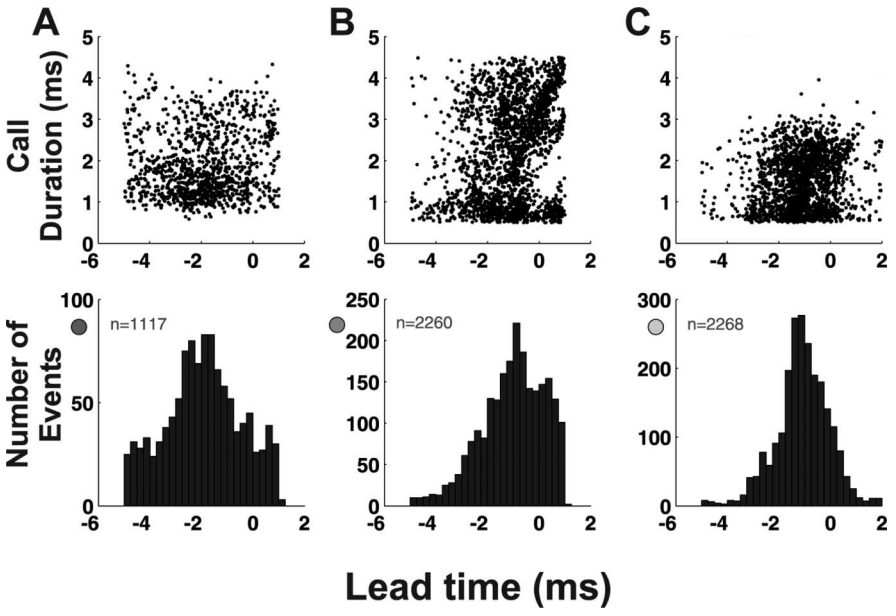

Figure 9. Short lead events are time locked well to sonar vocal onsets. Data in ***A–C*** are from three different randomly selected sites in three different bats and comprise all of the SLE data from single sessions. The short lead event data were collected while bats used echolocation to track a real oscillating target swinging toward and away from the bat. Top panels are sonar call duration versus short lead event times showing the uniform occurrence of event times with sonar call duration. Bottom row show histograms of the number of events at each time showing the precision of short lead events. Time bins are 0.25 ms. Values shown in bottom row represent the number of sonar calls used to construct each plot. Dots at the top of the ordinate, in the bottom row, draw attention to the different range of counts.

Third, given the small physical size of the SC, we examined the possibility that pre-vocal motor neural activity observed in the SC was generated in a separate structure but still observable in our SC recordings. Therefore, neural activity was recorded from the immediately adjacent and caudally situated IC while bats spontaneously produced sonar vocalizations. Neural recordings in the IC, using similar techniques to those described for SC recordings, revealed no LLE or SLE pre-vocal activity (Fig. 10*C*) ($n = 89$ sonar calls, single IC site). This was the case for all of our IC recording sites ($n = 5$). The rasters (Fig. 10*C*, top left) and PMTHs (Fig. 10*C*, bottom left) are aligned to sonar call onset ($t = 0$ ms), show no evidence of LLEs or SLEs, and have little overall activity before call onsets. Representative sonar call parameters produced during these trials (Fig. 10*C*, right column) show that the pulse interval, start and end frequency, and duration of emitted vocalizations in control experiments were comparable with those produced by the bat during the SC recordings (Figs. 6*B*,7*B*).

Fourth, we made EMG recordings from the muscles of mastication that lie on the dorsal surface of the head, adjacent to the chronic implant. These muscle groups flex when the animal moves its jaw, as during chewing or vocalizing, and the muscle EMG activity may contaminate the SC recordings. Vocal and neural recordings were made from two bats trained to spontaneously produce sonar vocalizations for variable periods of time (5–20 s) while resting on a platform. The peri-vocal rasters and PMTHs (Fig. 10*D*) show EMG activity in a 120 ms window around (100 ms before until 20 ms after) sonar call onsets ($n = 100$ sonar vocalizations). In contrast to the neural recordings in Figures 6 and 7, we observed no pattern of activity that was similar to the LLEs and SLEs observed in SC recordings. The event rate remained essentially constant (~50 events/s) and did not change in pattern before or after call onsets ($t = 0$ s).

Discussion

This study provides the first detailed report of vocal premotor activity in the superior colliculus of echolocating bats, animals that rely on acoustic orientation by sonar. Control studies exclude motor artifacts and demonstrate that neural activity in the bat SC precedes the production of sonar vocalizations and not communication calls. Furthermore, these findings are the first to demonstrate a relationship between the timing of premotor activity in the bat SC and the duration of an upcoming sonar cry.

Superior colliculus activity related to sonar vocalizations

Premotor activity in bat SC is consistently characterized by a temporally broad set of LLEs. In the goal-directed target tracking task, the $\langle LLE \rangle_{TIME}$ varies with sonar call duration, suggesting that SC premotor activity may serve to shape sonar vocal parameters for distance-dependent acoustic orienting. Adjustment of call duration with target distance has parallels with the control of depth of focus in primates and felines, which take place through vergence eye movements, accommodation, and pupillary constriction (Miles, 1985). Recent experiments suggest that the rostral pole of the SC in macaques plays a role in the control of vergence eye movements (Gnadt and Beyer, 1998; Chaturvedi and Van Gisbergen, 1999, 2000). Similar experiments conducted in cat also suggest a role for the rostral SC in accommodation and vergence eye movements (Suzuki et al., 2004). Therefore, call duration-dependent timing of LLE activity in bat SC might play a role in directing the distance-dependent changes in sonar cries that occur in foraging bats as they approach and attack insect prey (Surlykke and Moss, 2000).

Interestingly, no consistent relationship appeared between $\langle LLE \rangle_{TIME}$ and sonar call duration when bats were engaged in the virtual target amplitude discrimination task. We propose two explanations for why this pattern emerged only in the real oscillating target tracking task: (1) the target tracking task evoked a greater range of sonar cry durations in response to a greater range of target distances, thereby revealing the correlation, and/or (2) the tracking task directly engaged the bat in goal-directed behavior, which is required to shift $\langle LLE \rangle_{TIME}$ with call duration.

The precise premotor SLEs precede sonar vocalizations ~3 ms before vocal onset and with high temporal precision (SD <1.5 ms) (Figs. 6*A*, 7*A*). No consistent changes in the timing or event rate were observed for the SLE relative to sonar vocal duration or PI. SLE is too short to directly influence the upcoming sonar vocalization based on the number of estimated synapses between the SC and the laryngeal motor neurons (see below), but this premotor activity may serve other functions. For example, the SLEs may mark the timing of an impending sonar vocalization. This is important in echolocation behavior, which requires precise registration of call production time to accurately estimate echo delay, the bat's cue for target distance (Simmons, 1973).

There are two potential mechanisms whereby SLE activity could influence auditory responses to sonar vocalizations and echoes. *E. fuscus* vocalizations are intense, ~110–120 dB sound pressure level at 20 cm (Grinnell, 1963), which would severely mask detection of echoes (Moss and Schnitzler, 1995) if not for the following: (1) middle ear muscle contractions accompany vocalizations and thereby reduce hearing sensitivity to sonar cries (Suga and Jen, 1975), and (2) attenuation of auditory responses to sonar vocalizations, first observed in the lateral lemniscal nuclei (Suga and Schlegel, 1972). SLE activity may play a role in gating middle ear muscle contractions and neural attenuation that preserve auditory sensitivity to echoes. Additionally, SLE activity may shape the 3-D response profiles of auditory neurons in the bat SC (Valentine and Moss, 1997) by acting on local circuits that receive afferent input from the ascending lemniscal pathway (Huerta and Harting, 1984), the central acoustic tract (Casseday et al., 1989), and descending cortical inputs (Kobler et al., 1987).

In contrast to the consistent occurrence and precise timing of neural activity before sonar vocalizations, high-speed video data show no measurable relationship between the timing of head/pinna movements and SC neural activity. These findings do not exclude the possibility that head or pinna premotor activity is present in the bat SC, and two factors may account for their absence in our dataset. First, the experiments we conducted required the bat to direct its sonar along the range axis, minimizing lateral movements. Perhaps we would have observed premotor activity associated with head and/or pinna movements had the bats been engaged in tasks that required ballistic lateral orienting. It is also possible that our video sampling rate (250 frames/s) was not high enough to capture a relationship between pinna movements and premotor activity.

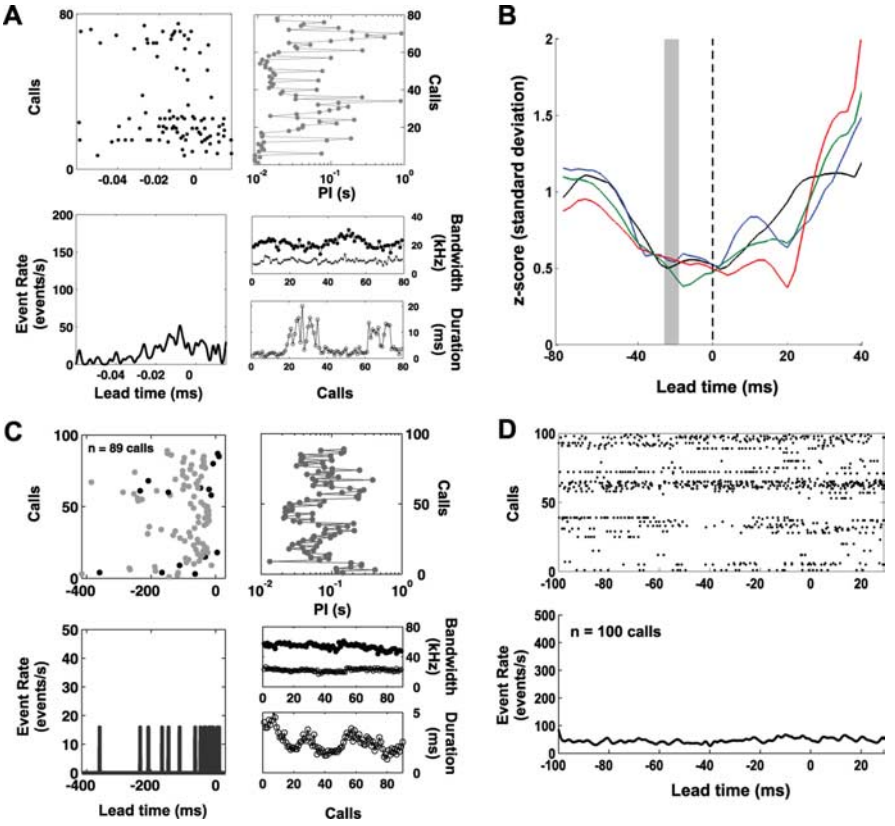

Figure 10. Control experiments conducted to verify relationship between SC premotor neural activity and sonar vocalizations. ***A***, Neural recordings were recorded simultaneously with non-sonar calls produced spontaneously by bats. Left, A raster plot and corresponding PMTHs do not show long lead events or short lead events when bats produce non-sonar calls. The raster and PMTHs show SC neural activity aligned with vocal onset ($t = 0$ ms) for $n = 79$ non-sonar calls from a single site. Right, Pulse interval, bandwidth, and call duration of non-sonar calls. ***B***, Head movements were tracked during the production of sonar vocalizations. The movement trajectories were normalized, to facilitate cross trial comparisons, using a *z*-score function. A reduction in the amount of head rotation precedes the expected time (gray bar) of premotor activity. The amount of head motion becomes increasingly variable at less reliable points in time after call onset. Data are from three bats (4 sessions), aligned to sonar call onset ($t = 0$ ms). Vertical gray bar represents mean time of long lead events ± 1 SD, as recorded in separate virtual target amplitude discrimination experiments. ***C***, No pre-vocal neural activity is observed in the inferior colliculus before sonar vocalizations. Gray dots represent the time of the last call, and black dots are event times. The PMTH shows low firing rates. Sonar pulse intervals range from 20 to 410 ms, similar to the range observed during virtual target discrimination experiments. Sonar call bandwidth, start frequencies (black, filled circles), and end frequencies (black, open circles) are shown for all of the sonar calls produced in this trial. ***D***, Raster and PMTH of electromyogram events recorded from the muscles of mastication on the dorsal surface of the skull. Events around sonar calls ($n = 100$ sonar calls) are aligned to call onset (lead time of $t = 0$ ms) and do not show deviations in rate before or after call onset. The event rate remains low (50 ± 5 events/s) around each sonar call onset.

Latency of vocal premotor activity

The event lead times we recorded in freely behaving animals are shorter than the latencies reported for vocalizations elicited by SC electrical stimulation in *E. fuscus* (63–170 ms; $n = 21$ sites) (Valentine et al., 2002) and *R. rouxi* (22–47 ms; $n = 103$ sites) (Schuller and Radtke-Schuller, 1990). The discrepancy may be attributable, in part, to the fact that sonar vocal production is coupled with respiration (Fattu and Suthers, 1981; Rübsamen and Schweizer, 1986; Schuller and Radtke-Schuller, 1990); therefore, sonar vocalization requires the coordinated recruitment of both respiratory and vocal motor pathways (Jürgens, 2002). Assuming

that microstimulation in the midbrain superior colliculus is an ineffective technique to appropriately recruit the respiratory motor pathway, the result may be a larger and longer range of latencies between electrical stimulation and vocal onset. It is also noteworthy that both species of bat can produce sonar vocalizations with short pulse intervals (<10 ms in *E. fuscus*; <10–50 ms in *R. rouxi*), requiring neural circuits that must operate on a similar timescale. The premotor activity we recorded in this study is more consistent with the temporal pattern of natural sonar vocal production, and the long latencies observed in SC electrical stimulation studies may not reflect the temporal dynamics of neural activity when bats are freely vocalizing.

Superior colliculus connections for sonar vocal control

Past research has implicated several brain regions in sonar vocal control. Experiments have primarily focused on loci in the ventral tegmentum and hindbrain in which microstimulation elicits and affects properties of sonar vocalizations (Rübsamen and Schweizer, 1986; Suga and Yajima, 1989; Metzner, 1996; Schuller et al., 1997; Fenzl and Schuller, 2002; Smotherman et al., 2003). Activity in these regions trigger sonar vocalizations and also influence the frequency and intensities of calls. In addition, microstimulation of the anterior cingulate cortex of the mustached bat (*Pteronotus parnelli*) reveals a topographic representation of sonar call frequency (Gooler and O'Neill, 1987).

The SC may participate in a vocal motor control circuit involving forebrain, thalamic, and midbrain and brainstem nuclei. For example, regions of the frontal cortex receiving projections from auditory cortex and suprageniculate nucleus project heavily onto the SC of *P. parnellii* (Kobler et al., 1987), potentially gating SC activity. In addition, the SC receives putative GABAergic projections from two nuclei, zona incerta in the medial thalamus and substantia nigra pars reticulata (Hikosaka and Wurtz, 1983; Nicolelis et al., 1992). Both projections may gate premotor activity in the SC and thereby control the timing and selection of orientation behaviors. The inhibitory projections from these regions may underlie the low background firing rates we observe in the SC, and disinhibition may explain the large and comparatively brief pre-vocal discharges.

The SC projects heavily onto the para-lemniscal area (PLa), a ventral tegmentum region that also receives substantial SC input (Schuller et al., 1997). In bat species that use constant frequency–FM echolocation signals and exhibit Doppler shift compensation behavior (Metzner, 1989; Schuller et al., 1997; Pillat and Schuller, 1998), the PLa plays a role in temporal and frequency control of sonar vocalizations. Neurons in the PLa respond to auditory stimuli and show modulation of their activity by the presence or absence of spontaneous vocalizations, and electrical stimulation of this brain region elicits sonar vocalizations (Metzner, 1989, 1993; Fenzl and Schuller, 2002). This is not the sole pathway for influencing sonar vocal production, because bats still produce sonar calls when the PLa is lesioned (Pillat and Schuller, 1998). In addition, the SC of *E. fuscus* shows anterograde projections to the parabrachial nucleus (S. Sinha, unpublished observations), which is implicated in the coordination of vocal production and respiration (Smotherman et al., 2006). This indirect tecto-tegmental pathway for influencing sonar vocalizations is similar to pathways implicated in mediating species-specific orienting behaviors in other animals (snakes, Gruberg et al., 1979; cats, Grantyn and Grantyn, 1982; turtles, Sereno, 1985; frogs, Masino and Grobstein, 1990; owl, Masino and Knudsen, 1992; primates, Scudder et al., 1996).

In summary, our study provides the first demonstration of SC premotor activity that accompanies the production of sonar vocalizations in echolocating bats. The vocal premotor activity shows distinct changes in temporal dynamics related to sonar call duration, which foraging bats adjust with target distance. Future experiments that expand on these findings in awake and freely behaving bats will serve to broaden our understanding of SC computations for the selection and execution of orienting behaviors.

References

Bankman IN, Johnson KO, Schneider W (1993) Optimal detection, classification, and superposition resolution in neural waveform recordings. IEEE Trans Biomed Eng 40:836–841.

Casseday JH, Kobler JB, Isbey SF, Covey E (1989) Central acoustic tract in an echolocating bat: an extralemniscal auditory pathway to the thalamus. J Comp Neurol 287:247–259.

Chaturvedi V, Van Gisbergen JA (1999) Perturbation of combined saccade-vergence movements by microstimulation in monkey superior colliculus. J Neurophysiol 81:2279–2296.

Chaturvedi V, Van Gisbergen JA (2000) Stimulation in the rostral pole of monkey superior colliculus: effects on vergence eye movements. Exp Brain Res 132:72–78.

Covey E, Hall WC, Kobler JB (1987) Subcortical connections of the superior colliculus in the mustache bat, *Pteronotus parnellii*. J Comp Neurol 263:179–197.

Dacey DM, Ulinski PS (1986) Optic tectum of the eastern garter snake, *Thamnophis sirtalis*. I. Efferent pathways. J Comp Neurol 245:1–28.

Dean P, Redgrave P, Westby GW (1989) Event or emergency? Two response systems in the mammalian superior colliculus. Trends Neurosci 12:137–147.

du Lac S, Knudsen EI (1990) Neural maps of head movement vector and speed in the optic tectum of the barn owl. J Neurophysiol 63:131–146.

Ewert JP (1997) Neural correlates of key stimulus and releasing mechanism: a case study and two concepts. Trends Neurosci 20:332–339.

Fattu JM, Suthers RA (1981) Subglottic pressure and the control of phonation by the echolocating bat, *Eptesicus fuscus*. J Comp Physiol 143:465–475.

Fenzl T, Schuller G (2002) Periaqueductal gray and the region of the paralemniscal area have different functions in the control of vocalization in the neotropical bat, *Phyllostomus discolor*. Eur J Neurosci 16:1974–1986.

Gnadt JW, Beyer J (1998) Eye movements in depth: what does the monkey's parietal cortex tell the superior colliculus? NeuroReport 9:233–238.

Gooler DM, O'Neill WE (1987) Topographic representation of vocal frequency demonstrated by microstimulation of anterior cingulate cortex in the echolocating bat, *Pteronotus parnelli parnelli*. J Comp Physiol A Neuroethol Sens Neural Behav Physiol 161:283–294.

Grantyn A, Grantyn R (1982) Axonal patterns and sites of termination of cat superior colliculus neurons projecting in the tecto-bulbo-spinal tract. Exp Brain Res 46:243–256.

Griffin DR (1958) Listening in the dark. New Haven: Yale UP.

Griffin DR, Webster FA, Michael CR (1960) The echolocation of flying insects by bats. Anim Behav 8:141–154.

Grinnell AD (1963) The neurophysiology of audition in bats: intensity and frequency parameters. J Physiol (Lond) 167:38–66.

Gruberg ER, Kicliter E, Newman EA, Kass L, Hartline PH (1979) Connections of the tectum of the rattlesnake *Crotalus viridis*: an HRP study. J Comp Neurol 188:31–41.

Guitton D, Munoz DP (1991) Control of orienting gaze shifts by the tectoreticulospinal system in the head-free cat. I. Identification, localization, and effects of behavior on sensory responses. J Neurophysiol 66:1605–1623.

Hartline PH, Kass L, Loop MS (1978) Merging of modalities in the optic tectum: infrared and visual integration in rattlesnakes. Science 199:1225–1229.

Hartridge H (1945) Acoustic control in the flight of bats. Nature 156:490–494.

Herrero L, Rodriguez F, Salas C, Torres B (1998) Tail and eye movements evoked by electrical microstimulation of the optic tectum in goldfish. Exp Brain Res 120:291–305.

Hikosaka O, Wurtz RH (1983) Effects on eye movements of a GABA agonist

and antagonist injected into monkey superior colliculus. Brain Res 272:368–372.
Hope GM, Bhatnagar KP (1979) Electrical response of bat retina to spectral stimulation: comparison of four microchiropteran species. Experientia 35:1189–1191.
Huerta MF, Harting JK (1984) The comparative neurology of the optic tectum, pp 687–773. New York: Plenum.
Jürgens U (2002) Neural pathways underlying vocal control. Neurosci Biobehav Rev 26:235–258.
Kobler JB, Isbey SF, Casseday JH (1987) Auditory pathways to the frontal cortex of the mustache bat, *Pteronotus parnellii*. Science 236:824–826.
Krauzlis RJ (2004) Recasting the smooth pursuit eye movement system. J Neurophysiol 91:591–603.
Masino T, Grobstein P (1990) Tectal connectivity in the frog *Rana pipiens*: tectotegmental projections and a general analysis of topographic organization. J Comp Neurol 291:103–127.
Masino T, Knudsen EI (1990) Horizontal and vertical components of head movement are controlled by distinct neural circuits in the barn owl. Nature 345:434–437.
Masino T, Knudsen EI (1992) Anatomical pathways from the optic tectum to the spinal cord subserving orienting movements in the barn owl. Exp Brain Res 92:194–208.
Metzner W (1989) A possible neuronal basis for Doppler-shift compensation in echolocating horseshoe bats. Nature 341:529–532.
Metzner W (1993) An audio-vocal interface in echolocating horseshoe bats. J Neurosci 13:1899–1915.
Metzner W (1996) Anatomical basis for audio-vocal integration in echolocating horseshoe bats. J Comp Neurol 368:252–269.
Miles FA (1985) Adaptive regulation in the vergence and accomodation control systems. In: Adaptive mechanisms in gaze control: facts and theories (Berthoz, Jones M, eds), pp 81–94. Amsterdam: Elsevier Science.
Moschovakis AK, Scudder CA, Highstein SM (1996) The microscopic anatomy and physiology of the mammalian saccadic system. Prog Neurobiol 50:133–254.
Moss CF (1998) Ontogeny of vocal signals in the big brown bat, *Eptesicus fuscus*. In: Animal sonar: processes and performance (Nachtigall PE, Moore PWB, eds), pp 115–120. New York: Plenum.
Moss CF, Schnitzler H-U (1995) Behavioral studies of auditory information processing. In: Hearing by bats, pp 87–145. Berlin: Springer.
Moss CF, Surlykke A (2001) Auditory scene analysis by echolocation in bats. J Acoust Soc Am 110:2207–2226.
Nicolelis MA, Chapin JK, Lin RC (1992) Somatotopic maps within the zona incerta relay parallel GABAergic somatosensory pathways to the neocortex, superior colliculus, and brainstem. Brain Res 577:134–141.
Pillat J, Schuller G (1998) Audiovocal behavior of Doppler-shift compensation in the horseshoe bat survives bilateral lesion of the paralemniscal tegmental area. Exp Brain Res 119:17–26.
Robinson DA (1972) Eye movements evoked by collicular stimulation in the alert monkey. Vision Res 12:1795–1808.
Rübsamen R, Schweizer H (1986) Control of echolocation pulses by neurons of the nucleus ambiguus in the rufous horseshoe bat, *Rhinolophus rouxi*. II. Afferent and efferent connections of the motor nucleus of the laryngeal nerves. J Comp Physiol A Neuroethol Sens Neural Behav Physiol 159:689–699.
Schuller G, Radtke-Schuller S (1990) Neural control of vocalization in bats: mapping of brainstem areas with electrical microstimulation eliciting species-specific echolocation calls in the rufous horseshoe bat. Exp Brain Res 79:192–206.
Schuller G, Fischer S, Schweizer H (1997) Significance of the paralemniscal tegmental area for audio-motor control in the moustached bat, *Pteronotus p. parnellii*: the afferent and efferent connections of the paralemniscal area. Eur J Neurosci 9:342–355.
Scudder CA, Moschovakis AK, Karabelas AB, Highstein SM (1996) Anatomy and physiology of saccadic long-lead burst neurons recorded in the alert squirrel monkey. I. Descending projections from the mesencephalon. J Neurophysiol 76:332–352.
Sereno MI (1985) Tectoreticular pathways in the turtle, *Pseudemys scripta*. I. Morphology of tectoreticular axons. J Comp Neurol 233:48–90.
Shimozawa T, Sun X, Jen PH (1984) Auditory space representation in the superior colliculus of the big brown bat, *Eptesicus fuscus*. Brain Res 311:289–296.
Simmons JA (1973) The resolution of target range by echolocating bats. J Acoust Soc Am 54:157–173.
Smotherman M, Zhang S, Metzner W (2003) A neural basis for auditory feedback control of vocal pitch. J Neurosci 23:1464–1477.
Smotherman M, Kobayasi K, Ma J, Zhang S, Metzner W (2006) A mechanism for vocal-respiratory coupling in the mammalian parabrachial nucleus. J Neurosci 26:4860–4869.
Sparks DL (2002) The brainstem control of saccadic eye movements. Nat Rev Neurosci 3:952–964.
Stein BE, Meredith MA (1993) The merging of the senses. Cambridge, MA: MIT.
Suga N, Jen PH (1975) Peripheral control of acoustic signals in the auditory system of echolocating bats. J Exp Biol 62:277–311.
Suga N, Schlegel P (1972) Neural attenuation of responses to emitted sounds in echolocating rats. Science 177:82–84.
Suga N, Yajima Y (1989) Auditory-vocal integration in the midbrain of the mustached bat: periaqueductal gray and the reticular formation. In: The physiological control of mammalian vocalization (Newman JD, ed), pp 87–107. New York: Plenum.
Surlykke A, Moss CF (2000) Echolocation behavior of big brown bats, Eptesicus fuscus, in the field and the laboratory. J Acoust Soc Am 108:2419–2429.
Suzuki S, Suzuki Y, Ohtsuka K (2004) Convergence eye movements evoked by microstimulation of the rostral superior colliculus in the cat. Neurosci Res 49:39–45.
Valentine DE, Moss CF (1997) Spatially selective auditory responses in the superior colliculus of the echolocating bat. J Neurosci 17:1720–1733.
Valentine DE, Sinha SR, Moss CF (2002) Orienting responses and vocalizations produced by microstimulation in the superior colliculus of the echolocating bat, *Eptesicus fuscus*. J Comp Physiol A Neuroethol Sens Neural Behav Physiol 188:89–108.
Wadsworth J, Moss CF (2000) Vocal control of acoustic information for sonar discriminations by the echolocating bat, *Eptesicus fuscus*. J Acoust Soc Am 107:2265–2271.